

# *Baseline Glass Development for Combined Fission Products Waste Streams*

**Advanced Fuel Cycle Initiative**

***Prepared for  
U.S. Department of Energy  
Waste Forms Campaign***

*J. V. Crum (PNNL), A. L. Billings  
(SRNL), J. Lang (PNNL), J. C. Marra  
(SRNL), C. Rodriguez (PNNL), J. V.  
Ryan (PNNL), J. D. Vienna (PNNL)*

***June 29, 2009***

**AFCI-WAST-WAST-MI-DV-2009-000075**

**PNNL-18524**



#### **DISCLAIMER**

This information was prepared as an account of work sponsored by an agency of the U.S. Government. Neither the U.S. Government nor any agency thereof, nor any of their employees, makes any warranty, expressed or implied, or assumes any legal liability or responsibility for the accuracy, completeness, or usefulness, of any information, apparatus, product, or process disclosed, or represents that its use would not infringe privately owned rights. References herein to any specific commercial product, process, or service by trade name, trade mark, manufacturer, or otherwise, does not necessarily constitute or imply its endorsement, recommendation, or favoring by the U.S. Government or any agency thereof. The views and opinions of authors expressed herein do not necessarily state or reflect those of the U.S. Government or any agency thereof.

## SUMMARY

A cost benefit analysis study recommended immobilization of the combined Cs/Sr/Ba/Rb (CS), lanthanide (LN) and transition metal fission product (TM) waste streams into a single borosilicate glass waste form.<sup>[1]</sup> Vitrification of the combined waste streams has a distinct advantage in terms of reduced infrastructure cost over treatment of individual waste streams. Borosilicate glass is also a proven technology, in terms of processing and wastefrom performance. Borosilicate glasses, similar to those proposed below, are currently the only accepted form for immobilization of U.S. high-level waste.

A joint study was undertaken at Pacific Northwest National Laboratory (PNNL) and Savannah River National Laboratory (SRNL) to develop acceptable glasses for the combined CS + LN + TM waste streams (Option 1) and CS + LN combined waste streams (Option 2) generated by the AFCI UREX+ set of processes. This study is aimed to develop baseline glasses for both combined waste stream options and identify key waste components and their impact on waste loading.

To identify the possible compositional envelope for the each of the combined waste streams options, elemental compositions of a “four-corners” study was used to determine the effect of burnup and decay on the fuel compositions. The four-corners study bracketed fuel burnup between a minimum of 25 gigawatt day per metric ton initial heavy metal (GWD/MTIHM) to a maximum of 100 GWD/MTIHM, with a center at 40 GWD/MTIHM, and decay time minimum of 5y and maximum of 50y, with a center of 10 years. The compositions of the individual waste streams generated by the UREX+ group of aqueous processes were then estimated based on available separations data<sup>[2-5]</sup>, noting that waste stream compositions are significantly impacted by the variability of the separations process. The waste stream impacted most was the TM fission products where Mo varies from 1.35 to 13.99 mass%, and noble metals vary from 0.96 to 19.60 mass%, on an oxide basis.

As a result, two different components/scenarios were identified that could limit waste loading of the combined CS + LN + TM waste streams: A high Mo scenario and a high noble metals scenario. In contrast, the combined CS + LN waste stream has no single component that is perceived to limit waste loading. Instead, a combined CS + LN waste stream in a glass waste form will likely be limited by heat because of the high activity of Cs and Sr isotopes.

A baseline glass was selected for each of the three extreme compositions:

1. Option 1 - High MoO<sub>3</sub> CS + LN + TM waste composition (referred to as Collins-CLT waste composition)
2. Option 1 - High noble metals CS + LN + TM waste composition (referred to as Bakel waste composition)
3. Option 2 - CS + LN waste composition (referred to as Collins-CL waste composition)

To select a baseline glass for Option 1 (high MoO<sub>3</sub>) five glasses were fabricated and tested in which the waste loading was varied to achieve a range of MoO<sub>3</sub> from 1.0 mass% to 3.5 mass%. Glass “CSLNTM-C-2.5” was selected as the baseline glass for the glass limited by high MoO<sub>3</sub>. Measured glass properties are summarized in Table S. This glass has the highest level of MoO<sub>3</sub>, at 2.5 mass%, where phase separation was not observed during melting or characterization. Second, though not a requirement but preferred, CSLNTM-C-2.5 was also the highest loaded glass that did not crystallize upon slow cooling. Lastly, the measured glass properties: T<sub>L</sub>, viscosity, electrical conductivity, and measured release rates of

the quenched and slow cooled glass were all well within the acceptable range for glass processing and waste form performance.

Option 1 Glass “CSLNTM-B-3.0” was fabricated and tested as the baseline glass for the glass limited by high noble metals. The glass was formulated and fabricated at the current processing limit of 3 mass% noble metals. Measured glass properties are summarized in Table S. This glass crystallized 7 mass % of calcium neodymium silicate ( $\text{Ca}_2\text{Nd}_8\text{Si}_6\text{O}_{26}$ ) upon slow cooling. The slow cooled glass still performed as well or better than the quenched glass as tested by the PCT. The measured glass properties  $T_L$ , viscosity, electrical conductivity, and measured release rates of the quenched and slow cooled glass were all well within the acceptable range for glass processing and waste form performance.

Four Option 2 glasses were fabricated, where the waste loading and glass formers  $\text{Al}_2\text{O}_3$ ,  $\text{B}_2\text{O}_3$ , and  $\text{SiO}_2$ , were varied. Glass “CSLN-7C” was selected as the baseline for the Option 2 (CS + LN only) glasses fabricated and tested based on its overall properties, as shown in Table S. This glass had the lowest measured  $T_L$  ( $\sim 1200^\circ\text{C}$ ), which was  $100\text{--}200^\circ\text{C}$  lower than the other three glasses tested. The low  $T_L$  allows the melter operating temperature to be dropped accordingly, which generally results in lower  $\text{Cs}_2\text{O}$  volatility, as was observed based on the measured compositions of the fabricated glasses. This glass has a low electrical conductivity because of the low concentration of alkali, at 2.66 mole%.

The other three Option 2 glasses tended to massively crystallize upon slow cooling as the waste loading was increased. Consequently, the development of a glass-ceramic waste form would be a logical approach to achieve higher waste loading for the combined CS + LN waste stream. If a glass-ceramic was developed that was  $> 90$  mass% crystallized, then heat load would not be limited by the  $T_g$  but by the higher melting points of the crystalline phases or the container.

It should be noted that while borosilicate based glass was selected as the baseline glass for this study, that the phosphate glass system is currently being examined by others for the Option 1 high  $\text{MoO}_3$  combined waste stream to determine if it might be a better glass system for high  $\text{MoO}_3$ .

Table S Summary of glass properties

Glass ID	CSLNTM-C-2.5	CSLNTM-B-3.0	CSLN-7C
Quenched crystallinity, mass%	Trace $\text{RuO}_2$	Trace $\text{RuO}_2$	0
Slow cooled crystallinity, mass%	Trace $\text{RuO}_2$	7.0, $\text{Ca}_2\text{Nd}_8\text{Si}_6\text{O}_{26}$ Trace $\text{RuO}_2$	0
Optical $T_L$ , $^\circ\text{C}$	1017	1128	1208
XRD $T_L$ , $^\circ\text{C}$	1030	1141	NA
Primary crystalline phase	$\text{Ca}_2\text{Nd}_8\text{Si}_6\text{O}_{26}$	$\text{Ca}_2\text{Nd}_8\text{Si}_6\text{O}_{26}$	
Quenched PCT B, g/L	0.21	0.25	0.04
Slow cooled PCT B, g/L	0.19	0.18	0.02
Density, $\text{g/cm}^3$	2.78	2.89	3.36
$T_g$ , $^\circ\text{C}$	515	527	719
$T_M$ , $^\circ\text{C}$	1233	1240	1356
$A^{(a)}$	-8.68	-10.35	-19.00
$B^{(a)}$	15505	18097	33582
$\epsilon$ at $T_M$ , S/m	20.53	17.21	0.71
$C^{(b)}$	8.42	9.02	17.58
$D^{(b)}$	-8124	-9338	-29201

(a)  $\text{Ln}[\eta, \text{Pa-s}] = A + B/T$

(b)  $\text{Ln}[\epsilon, \text{S/m}] = C + D/T$

## CONTENTS

SUMMARY .....	1
ACRONYMS .....	5
1. INTRODUCTION.....	6
2. Objectives .....	8
3. Experimental .....	10
3.1 Glass Fabrication.....	10
3.2 Slow Cool Heat Treatment .....	11
3.3 Glass Testing (Property Measurements).....	11
3.3.1 Compositional Analysis .....	11
3.3.2 Product Consistency Test (PCT) Response.....	11
3.3.3 Homogeneity as Defined by X-Ray Diffraction (XRD) Analysis .....	11
3.3.4 Liquidus Temperature ( $T_L$ ).....	12
3.3.5 Density .....	12
3.3.6 Glass Transition temperature ( $T_g$ ).....	12
3.3.7 Viscosity.....	12
4. Results .....	13
4.1 Observations of As-Fabricated Glasses .....	13
4.2 Slow Cooled Glasses .....	15
4.3 Chemical Composition Results .....	18
4.4 PCT Results .....	20
4.5 Liquidus Temperature.....	22
4.6 Measured Glass Density and Glass Transition Temperature .....	24
5. Conclusions.....	25
6. References.....	26
Appendix A Slow Cooling Heat Treatment Curve.....	28

## FIGURES

Figure 1 Photo of CSLNTM-C-2.5 as-fabricated glass from 2 <sup>nd</sup> melt pour patty .....	13
Figure 2 XRD scans of Option 1 glasses with fluorite internal standard.....	14
Figure 3 XRD scans of Option 2 glasses with fluorite internal standard.....	14
Figure 4 Pictures of Option 1 glasses following slow cooled heat treatment. ....	15
Figure 5 Pictures of Option 2 glasses following slow cooled heat treatment. ....	16
Figure 6 XRD scans of slow cooled Option 1 glasses (used corundum as internal standard when crystals were present).....	17

Figure 7 XRD scans of slow cooled Option 1 glasses (used corundum as internal standard when crystals were present).....	18
Figure 8 CSLNTM-C-2.5 at 998°C for 24 hr containing $\text{Ca}_{2.2}\text{Nd}_{7.8}\text{Si}_6\text{O}_{26}$ (center) and RuO <sub>2</sub> undissolved particles (throughout).....	23
Figure 9 CSLNTM-C-1.5 heat-treated at 850°C containing $\text{Ca}_{2.2}\text{Nd}_{7.8}\text{Si}_6\text{O}_{26}$ (center), RuO <sub>2</sub> needles and undissolved particles (throughout).....	23
Figure 10 CSLN-5 heat-treated at 1300°C.....	24

## TABLES

Table S Summary of measured glass properties .....	2
Table 1 Composition estimates (in mass percent oxide) of the CS/LN and CS/LN/TM waste stream combinations (each estimate is based on LWR fuel after 40 GWd burn-up and 10 year decay storage) .....	7
Table 2 Option 1 glass compositions in terms of mass percent oxide .....	9
Table 3 Option 2 glass compositions in mass percent oxide .....	10
Table 4 Slow cooling heat treatment schedule.....	16
Table 5 Crystalline phases present after slow cooling with quantitative or qualitative concentrations.....	17
Table 6 Option 1 measured and target glass compositions, mass% .....	19
Table 7 Option 2 measured and target glass compositions, mass% .....	20
Table 8 Measured PCT response for Option 1 quenched and slow cooled glasses.....	21
Table 9 Measured PCT response for Option 2 quenched and slow cooled glasses.....	21
Table 10 Optical and XRD measured $T_L$ of the Option 1 and 2 glasses along with primary crystalline phase <sup>(b)</sup> .....	22
Table 11 Measured densities of Option 1 and 2 glasses .....	24
Table 12 Summary of measured glass properties.....	25

## ACRONYMS

AFCI	Advanced Fuel Cycle Initiative
ARM	Approved Reference Material
ASTM	American Standards and Testing Methods, now ASTM International, Inc.
CS	alkaline / alkaline earth fission products
DOE	U.S. Department of Energy
DTA/TGA	differential temperature analysis / thermal galvanometric analysis
EA	environmental assessment
ICCD	International Center of Crystallographic Data
ICP-AES/MS	inductive coupled plasma - atomic emissions spectroscopy / mass spectrometer(ry)
ICSD	International Center of Structure Data
LaBS	lanthanide borosilicate
LDRD	Laboratory Directed Research and Development
LN	lanthanide fission products
OM	optical microscope(y)
PCT	product consistency test
PNNL	Pacific Northwest National Laboratory
SRNL	Savannah River National Laboratory
SNF	spent nuclear fuel
SEM-EDS	scanning electron microscope(y) – energy dispersive spectroscopy
T <sub>g</sub>	glass transition temperature
T <sub>L</sub>	liquidus temperature
T <sub>M</sub>	glass melting temperature
TM	transition metal fission products
UREX	uranium extraction process
Vol-Ox	volatilization-oxidation
XRD	X-ray diffraction

## 1. INTRODUCTION

This study was undertaken as a joint effort by Pacific Northwest National Laboratory (PNNL) and Savannah River National Laboratory (SRNL) to develop acceptable glass waste forms for two potential combined waste streams from the Advanced Fuel Cycle Initiative (AFCI) aqueous separations process. The AFCI is a program sponsored by U.S. Department of Energy (DOE) to develop and demonstrate a process for the recycling of spent nuclear fuel (SNF). The process generates several secondary streams that require disposition in acceptable waste forms. Glass was selected as the preferred option for immobilization of a combination of most or all of the Cs/Sr/Ba/Rb (CS), lanthanide fission product (LN), and transition metal fission product (TM) waste streams from the AFCI separations process as a result of a recent cost benefit analysis study.<sup>[1]</sup>

This study will focus on the development of acceptable glass wasteforms for two possible waste stream combinations:

- CS + LN (CS/LN)
- CS + LN + TM (CS/LN/TM)

with most of the focus being on the latter. Composition estimates of these waste stream combinations as oxides are given in Table 1. The combined waste stream is dominated by lanthanides,  $\text{ZrO}_2$ , alkalis, alkaline earths,  $\text{MoO}_3$ , and noble metals ( $\text{PdO}$ ,  $\text{Rh}_2\text{O}_3$ , and  $\text{RuO}_2$ ). As illustrated in Table I, a wide range of possible quantities are shown for several of the elements in the CS/LN/TM waste stream because of the following variability in:

- Volatile-oxidation (Vol-Ox) separations efficiency (for noble metals)
- Partitioning of noble metals to undissolved solids
- Mo and Zr content in the undissolved solids
- The amount of Zr-molybdates precipitated during processing

As a result of variations in these quantities among the investigated literature,<sup>[2-5]</sup> the waste stream concentrations of  $\text{MoO}_3$  have been predicted to vary from 1.35 to 13.99 mass%,  $\text{ZrO}_2$  from 3.04 to 13.75 mass%, and noble metals from 0.96 to 19.60 mass%. For the benefit of this study, (or to facilitate this study) two example waste compositions were chosen that are believed to represent endpoint possibilities expected from the separations process.<sup>[2,5]</sup> In addition, the most recent study by Collins was the first to provide results of the volatilization-oxidation (Vol-Ox) process on noble metal partitioning to the off-gas,<sup>[5]</sup> which may be implemented in the final flowsheet. To account for this, the 50 percent reduction in Ru and Rh that was observed for the Vol-Ox process has been applied to both of the reference CS/LN/TM waste compositions.<sup>[2,5]</sup> For more details about the calculated waste compositions see the complete description of the assumptions and calculations.<sup>[6]</sup>



Table 1 Composition estimates (in mass percent oxide) of the CS/LN and CS/LN/TM waste stream combinations (each estimate is based on LWR fuel after 40 GWd burn-up and 10 year decay storage)

Author:	Collins-CL <sup>[5]</sup>	Collins-CLT <sup>[5]</sup>	Bakel <sup>[2]</sup>
Waste Stream Combination:	CS/LN	CS/LN/TM	CS/LN/TM
SeO <sub>2</sub>	-	0.29	0.32
Br	-	0.08	0.09
Rb <sub>2</sub> O	2.22	1.50	1.63
SrO	5.14	3.49	3.77
Y <sub>2</sub> O <sub>3</sub>	0.49	2.23	2.41
ZrO <sub>2</sub>	-	10.60	3.33
MoO <sub>3</sub>	-	13.88	3.00
RuO <sub>2</sub>	-	0.70	6.20
Rh <sub>2</sub> O <sub>3</sub>	-	0.28	1.21
PdO	-	0.06	5.73
AgO <sub>2</sub>	-	0.40	0.43
CdO	-	0.39	0.43
In <sub>2</sub> O <sub>3</sub>	-	0.01	0.01
SnO <sub>2</sub>	-	0.25	0.27
Sb <sub>2</sub> O <sub>3</sub>	-	0.04	0.05
TeO <sub>2</sub>	-	2.33	2.52
Cs <sub>2</sub> O	15.08	10.22	11.05
BaO	11.55	7.83	8.47
La <sub>2</sub> O <sub>3</sub>	8.21	5.62	6.08
Ce <sub>2</sub> O <sub>3</sub>	15.28	11.01	11.91
Pr <sub>2</sub> O <sub>3</sub>	7.51	5.14	5.56
Nd <sub>2</sub> O <sub>3</sub>	27.11	18.56	20.07
Pm <sub>2</sub> O <sub>3</sub>	0.08	0.06	0.06
Sm <sub>2</sub> O <sub>3</sub>	5.58	3.82	4.13
Eu <sub>2</sub> O <sub>3</sub>	0.89	0.61	0.66
Gd <sub>2</sub> O <sub>3</sub>	0.84	0.57	0.62
Tb <sub>2</sub> O <sub>3</sub>	0.02	0.01	0.01
Total, g/MTIHM <sup>a</sup>	20,853.88	30,765.56	30,609.03

<sup>a</sup> MTIHM: metric ton initial heavy metal

### Option 1

Borosilicate and/or phosphate glass systems were identified as likely candidates for immobilization of the combined CS/LN/TM waste stream because of the complex chemical composition of the waste and the high variability of  $\text{MoO}_3$ , noble metals, and  $\text{ZrO}_2$ . Advantages of borosilicate glass include the vast amount of prior research as a waste form for defense waste processing,<sup>[7-9]</sup> demonstrated large scale processing and, with the exceptions of  $\text{MoO}_3$  and noble metals, the high solubility of all other components in the waste stream. The main disadvantage of borosilicate glass as a waste form is the relative insolubility of  $\text{MoO}_3$ , which tends to form a separated Mo-rich phase at concentrations higher than 1 to 3 mass%. Noble metals are also very insoluble in this glass and provide a highly conductive phase within that may cause significant processing problems. It should be noted that the amount at which the noble metals will cause processing difficulty is not clearly defined and will depend on the melter technology and processing methods employed.

Alternatively, phosphate glasses have been shown to accommodate high concentrations of  $\text{LN}_2\text{O}_3$ , alkalis, alkaline earths, and  $\text{MoO}_3$ .<sup>[10]</sup> However, possible shortcomings include much less robust composition and lower amount of literature attention, possible limited solubility of  $\text{ZrO}_2$ , lower glass transition temperatures ( $T_g$ ), and similar problems regarding noble metals as the borosilicate glass waste form.

### Option 2

A modified version of lanthanide borosilicate (LaBS) glass was identified as a good candidate for immobilization of the CS/LN combined waste stream, because the potential waste stream essentially consists of alkali, alkaline earth, and rare earth oxides. The LaBS glass has been shown to accept extremely high loadings, up to 62.5 mass%, of  $\text{Ln}_2\text{O}_3$  with acceptable melter processing properties and good product performance.<sup>[11-14]</sup> The studies conclude that waste loading was ultimately limited by liquidus temperature which is linked to  $\text{Ln}_2\text{O}_3$  concentration. A prior PNNL Laboratory Directed Research and Development (LDRD) study generated four glass compositions based on a modified LaBS glass that will be incorporated into the current study.<sup>[15]</sup>

## **2. Objectives**

The objective of this study is to develop acceptable baseline glass waste forms for the immobilization of the combined CS/LN/TM (Option 1) and CS/LN waste streams (Option 2). In order to facilitate the selection of a baseline composition, a series of glass compositions were chosen and synthesized based on the current data and available glass property models available.

### Option 1

The available data and property models for borosilicate and phosphate glasses do not directly address the anticipated compositions. At required levels of waste loading, these glasses would contain significantly higher concentrations of  $\text{MoO}_3$ ,  $\text{ZrO}_2$ , and/or noble metals than have been previously studied. Five glass compositions were explored in the borosilicate glass system to identify baseline glasses appropriate for each of the high  $\text{MoO}_3$  waste stream compositions and one glass for the high noble metals waste stream composition possibilities (e.g., Collins and Bakel), as shown in Table 2. The first part of the glass ID denotes the combined waste streams followed by either a C for Collins-CLT (high  $\text{MoO}_3$ ) or B for Bakel (high noble metals). The number at the end of each glass ID refers to the level of  $\text{MoO}_3$  or noble metal respectively.

Table 2 Option 1 glass compositions in terms of mass percent oxide

Components	CSLNTM-C-1	CSLNTM-C-1.5	CSLNTM-C-2	CSLNTM-C-2.5	CSLNTM-C-3.5	CSLNTM-B-3.0
Ag <sub>2</sub> O	0.03	0.04	0.06	0.07	0.10	0.11
Al <sub>2</sub> O <sub>3</sub>	10.00	9.38	6.66	5.95	5.68	6.53
B <sub>2</sub> O <sub>3</sub>	10.00	9.65	8.46	5.00	5.00	5.16
BaO	0.56	0.85	1.13	1.41	1.98	2.20
CaO	5.00	5.00	5.00	7.00	5.00	5.16
CdO	0.03	0.04	0.06	0.07	0.10	0.11
Ce <sub>2</sub> O <sub>3</sub>	0.79	1.19	1.59	1.98	2.78	3.09
Cs <sub>2</sub> O	0.74	1.10	1.47	1.84	2.58	2.87
Eu <sub>2</sub> O <sub>3</sub>	0.04	0.07	0.09	0.11	0.15	0.17
Gd <sub>2</sub> O <sub>3</sub>	0.04	0.06	0.08	0.10	0.15	0.16
La <sub>2</sub> O <sub>3</sub>	0.40	0.61	0.81	1.01	1.42	1.58
Li <sub>2</sub> O	4.50	4.50	4.50	4.02	3.30	3.21
MoO <sub>3</sub>	<b>1.00</b>	<b>1.50</b>	<b>2.00</b>	<b>2.50</b>	<b>3.50</b>	0.78
Na <sub>2</sub> O	8.37	7.00	6.00	7.00	7.00	7.22
Nd <sub>2</sub> O <sub>3</sub>	1.34	2.01	2.68	3.36	4.70	5.22
PdO	0.00	0.01	0.01	0.01	0.02	<b>0.02</b>
Pr <sub>2</sub> O <sub>3</sub>	0.37	0.56	0.74	0.93	1.30	1.44
Rb <sub>2</sub> O	0.11	0.16	0.22	0.27	0.38	0.42
RhO <sub>2</sub>	0.02	0.03	0.04	0.05	0.07	<b>0.07</b>
RuO <sub>2</sub>	0.05	0.08	0.10	0.13	0.18	<b>0.18</b>
SeO <sub>2</sub>	0.02	0.03	0.04	0.05	0.07	0.08
SiO <sub>2</sub>	54.93	53.67	54.98	53.03	48.82	49.94
Sm <sub>2</sub> O <sub>3</sub>	0.28	0.41	0.55	0.69	0.96	1.07
SnO <sub>2</sub>	0.02	0.03	0.04	0.04	0.06	0.07
SrO	0.25	0.38	0.50	0.63	0.88	0.98
TeO <sub>2</sub>	0.17	0.25	0.34	0.42	0.59	0.65
Y <sub>2</sub> O <sub>3</sub>	0.16	0.24	0.32	0.40	0.56	0.63
ZrO <sub>2</sub>	0.76	1.15	1.53	1.91	2.67	0.87
Sum	100.00	100.00	100.00	100.00	100.00	100.00
Waste Loading	7.20	10.81	14.41	18.01	25.22	25.15

In the case of CSLNTM-B-3.0, the glass (based on Bakel waste composition, from Table 1) was formulated with three mass% combined noble metals (RhO<sub>2</sub>, RuO<sub>2</sub>, and PdO); however, for the purposes of making a glass for testing, the noble metals were partially removed by normalizing only the noble metals down to same levels as CSLNTM-C-3.5. This was done to make the glass less expensive. Past crucible-scale tests with noble metals at very high concentrations either separate to the crucible bottom or remain trapped along the top walls of the crucible as the batch melts and thus are not distributed throughout the glass.

The phosphate glass system is being investigated at the Mo-SCI Corporation and will be documented in a separate report.

### Option 2

Limited effort was spent on Option 2 as the TM are currently more economically immobilized in a glass than in a metal waste form. The costs of these two options, however, are uncertain enough to warrant some effort to establish a baseline CS/LN glass so that subsequent cost-benefit trade studies will be sufficiently detailed as to make an accurate comparison. As such, four glasses were formulated, fabricated, and tested to supplement the available LDRD data, with compositions shown in Table 3.<sup>[15]</sup>

Table 3 Option 2 glass compositions in mass percent oxide

oxide	CSLN-5	CSLN-6	CSLN-7	CSLN-8
Al <sub>2</sub> O <sub>3</sub>	17.00	17.00	17.00	20.00
B <sub>2</sub> O <sub>3</sub>	10.00	5.00	10.00	10.00
BaO	6.98	7.61	5.71	6.98
Ce <sub>2</sub> O <sub>3</sub>	8.61	9.39	7.04	8.61
Cs <sub>2</sub> O	7.31	7.97	5.98	7.31
Eu <sub>2</sub> O <sub>3</sub>	0.50	0.54	0.41	0.0050
Gd <sub>2</sub> O <sub>3</sub>	0.57	0.62	0.46	0.57
La <sub>2</sub> O <sub>3</sub>	4.39	4.79	3.59	4.39
Nd <sub>2</sub> O <sub>3</sub>	14.50	15.82	11.86	14.50
Pr <sub>2</sub> O <sub>3</sub>	4.00	4.37	3.28	4.00
Rb <sub>2</sub> O	0.94	1.02	0.77	0.94
SiO <sub>2</sub>	18.00	18.00	28.00	15.00
Sm <sub>2</sub> O <sub>3</sub>	3.04	3.32	2.49	3.04
SrO	2.41	2.63	1.98	2.41
Y <sub>2</sub> O <sub>3</sub>	1.75	1.91	1.43	1.75
Total	100.00	100.00	100.00	100.00
Waste Loading	55.00	60.00	45.00	55.00

## 3. Experimental

### 3.1 Glass Fabrication

Glasses were batched and melted according to PNNL Procedure GDL-GBM, Rev. 3.<sup>[16]</sup> Each glass batch was prepared by first weighing out the proper mass of each reagent-grade chemical in the form of metal oxides, carbonates, H<sub>3</sub>BO<sub>3</sub>, and salts. Each batch was 500 grams in size to produce enough glass for the associated testing and to minimize compositional errors associated with weighing out minor components. Batches were then homogenized by placing them into an agate milling chamber consisting of an agate puck and chamber. The chamber was then placed into the pulverizer mill (Angstrom Inc., Belleville, MI) and ground/mixed for four minutes. The milled batch was then placed into a platinum-rhodium crucible with a lid that was placed into a high temperature furnace for 1 h at the predicted melting temperature (T<sub>M</sub>), at which the viscosity = 5 Pa·s. If necessary, the temperature was adjusted after ~15 min of melting time, to achieve a fluid melt with a viscosity of 5±3 Pa·s. The melts were then quenched by casting them onto clean stainless steel plates. After visual examination, small samples were removed and saved for

glasses with any unique features such as phase separation or undissolved materials. The glass was then placed into a tungsten carbide milling chamber that consist of a puck, ring, and chamber and ground for 4 min. This process typically grinds the glass homogenizes the powder with a particle size of roughly 1-50  $\mu\text{m}$ . The glass was then remelted for an hour and again quenched on the stainless steel plate. Final visual observations of the glass were recorded for the quenched glass.

## 3.2 Slow Cool Heat Treatment

Slow cooled heat treatments were performed by placing ~ 20 g of as-fabricated glass into a platinum-rhodium crucible with lid. Specimens were then loaded into a furnace at a temperature of 1150°C for 30 minutes to form a melt, followed by a series of progressively slower ramp rates to simulate canister centerline cooling rates.

## 3.3 Glass Testing (Property Measurements)

The following subsections describe the chemical and physical property measurements made on each glass or select glasses.

### 3.3.1 Compositional Analysis

To confirm that the “as-fabricated” glasses matched the defined target compositions, a representative sample of each glass was chemically analyzed. Two samples of each glass to be analyzed were fused separately in KOH and/or  $\text{Na}_2\text{O}_2$  and the fused mass dissolved in dilute  $\text{HNO}_3$ -HF for analysis with Inductively Coupled Plasma – Atomic Emission Spectroscopy/Mass Spectrometry (ICP-AES/MS).<sup>[17-19]</sup> Glass standards were also tested throughout each set of samples to assess the performance of the ICP-AES/MS over the course of these analyses. Also, because of concerns with the possibility of a separated molybdate-containing phase, glass samples were rinsed with 10 mL of DI water and passed through a 60  $\mu\text{m}$  filter. The solutions were then analyzed with ICP-AES/MS in order to determine if a readily soluble phase was present.

### 3.3.2 Product Consistency Test (PCT) Response

The PCT was performed in triplicate on glasses as a measure of chemical durability according to American Standard Test Methods International (ASTM) C-1285-2002.<sup>[20]</sup> Test method “A” in the protocol was followed. Also included in the experimental test matrix were the Environmental Assessment (EA) glass, the Approved Reference Material (ARM) glass, and blanks. Samples were ground, washed, and prepared according to procedure.<sup>[20]</sup> At the conclusion of the seven-day test the resulting solutions (leachates) of the glasses and standards were analyzed with the appropriate analytical method (i.e., ICP-AES/MS) for Al, Si, B, Na, Mo, and Li release. The analyte concentrations were normalized for the concentration of those elements in glass (based on measured compositions).

### 3.3.3 Homogeneity as Defined by X-Ray Diffraction (XRD) Analysis

Representative samples of as-fabricated and slow cooled glass were analyzed with XRD to determine the types and quantities of crystals formed.<sup>[21,22]</sup> Samples were spiked with a known mass of an internal standard to calibrate the peak locations and integrated intensities for phase identification and quantification. Identification and/or quantification of crystal fractions in the samples were done if structure files were available in the International Center of Crystallographic Data (ICCD) and International Center of Structure Data (ICSD) data bases or literature.

### 3.3.4 Liquidus Temperature ( $T_L$ )

Liquidus temperature ( $T_L$ ) was measured according to Methods B and C of PNNL Procedure GDL-LQT, Rev. 4.<sup>[22]</sup> The equilibrium crystal fraction as a function of temperature was measured by heat treating specimens in Pt-alloy crucibles with tight fitting lids to minimize volatilization. The heat treatment times varied from 4-72 h to ensure equilibrium was achieved without excessive volatility near the melting temperature. Samples were quenched and analyzed to determine the type and quantity of crystal fractions (quantitative analyses). The temperatures were varied so that the temperatures corresponding to between 0.5 and 3 vol% crystals can be calculated, if possible, and also so that the temperature at 0 vol% crystals can be narrowed to within 10°C. Samples were also thin-sectioned and examined with optical microscopy to identify the presence of crystals and determine  $T_L$ . A standard glass, NBS-773, was measured for data validation.

### 3.3.5 Density

Densities of the glasses were measured with the helium pycnometry according to PNNL procedure GDL-PYC Rev 2.<sup>[23]</sup> Samples were prepared, cleaned and dried, according to procedure. Each specimen mass was measured on a calibrated balance with accuracy to 0.2mg and then loaded into the helium pycnometer to measure the sample volume. The pycnometer was calibrated according to the manufacturer's procedure with a supplied WC ball of known volume.

### 3.3.6 Glass Transition temperature ( $T_g$ )

The  $T_g$  was measured with DTA/TGA and dilatometry at PNNL according to ASTM E1356-08 and ASTM E 1545-05.<sup>[24,25]</sup>

### 3.3.7 Viscosity

For the baseline glasses, viscosity was measured as a function of temperature over a viscosity range of 5 to 200 P $\cdot$ s according to PNNL procedure GDL -VIS.<sup>[26]</sup> About 50 ml of glass was placed into a cylindrical crucible and melted. A platinum spindle was lowered into the glass melt. The spindle was attached to a rotating viscometer head that controlled speed and measured torque. Speed, torque, and spindle factor (determined by calibration) were used to calculate viscosity of the glass at several different temperatures.



## 4. Results

### 4.1 Observations of As-Fabricated Glasses

All of the glasses melted and poured easily. Glass CSLNTM-C-3.5 formed a separated liquid phase that was observed upon pouring after the first 1 hr melt. The phase appeared to be a molybdate. However the separated phase was reincorporated into the glass during the second 1 hr melt. After the second melt, all of the Option 1 glasses were transparent with a light to dark green color and small undissolved  $\text{RuO}_2$  particles. Option 2 glasses were homogenous and crystal free after the second melt. Samples of the Option 1 glasses were thin-sectioned and examined by optical microscopy for evidence of crystalline phases and phase separation. All of the Option 1 glasses contained undissolved  $\text{RuO}_2$  similar to those shown in Figure 1. There was no evidence of any other crystalline phases or phase separation observed with optical microscopy (OM) in the thin-sections.

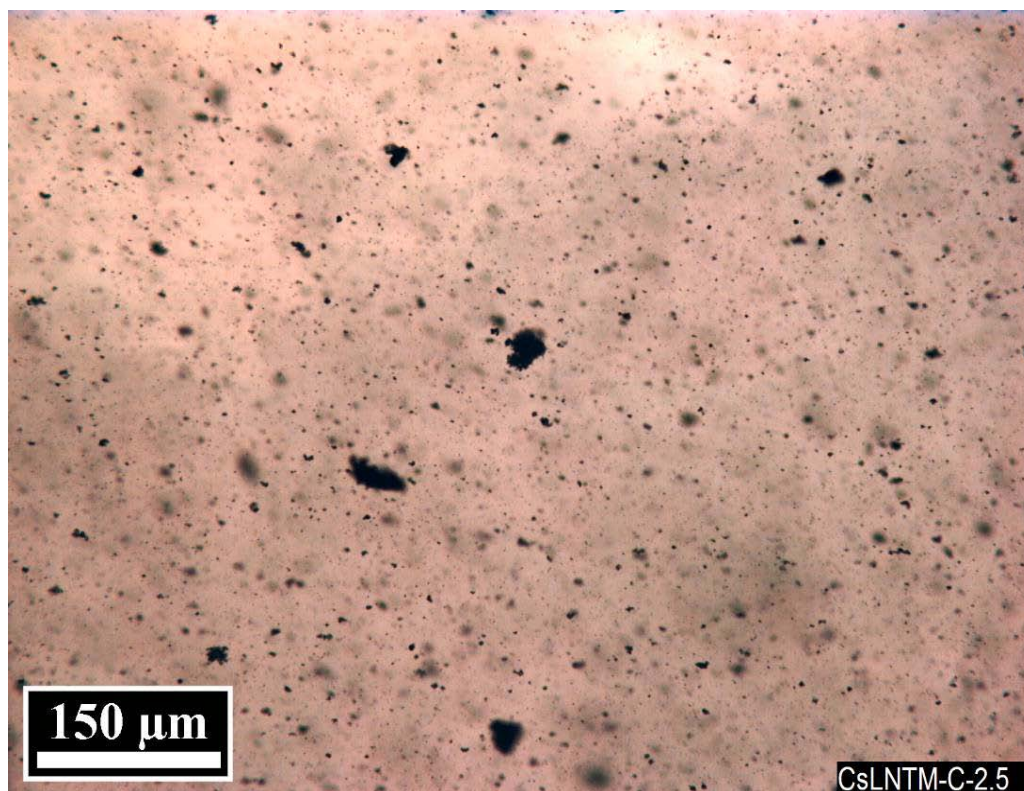


Figure 1 Optical transmitted light micrograph of CSLNTM-C-2.5 as-fabricated glass from 2<sup>nd</sup> melt pour patty.

The as-fabricated glasses were each spiked with a known mass of an internal fluorite standard and examined with XRD to identify crystalline phases. For Option 1 glasses, CSLNTM-C-1.0, 1.5 and 2.0 appeared completely amorphous, while CSLNTM-C-2.5, 3.5 and CSLNTM-B-3.0 contained trace amounts of  $\text{RuO}_2$ , shown in Figure 2. The presence of  $\text{RuO}_2$  was expected, as it is insoluble in glass and has been observed in glass waste forms for the combined LN + TM waste streams.<sup>[27]</sup> All of the Option 2 glasses were completely X-ray amorphous, as shown in Figure 3.

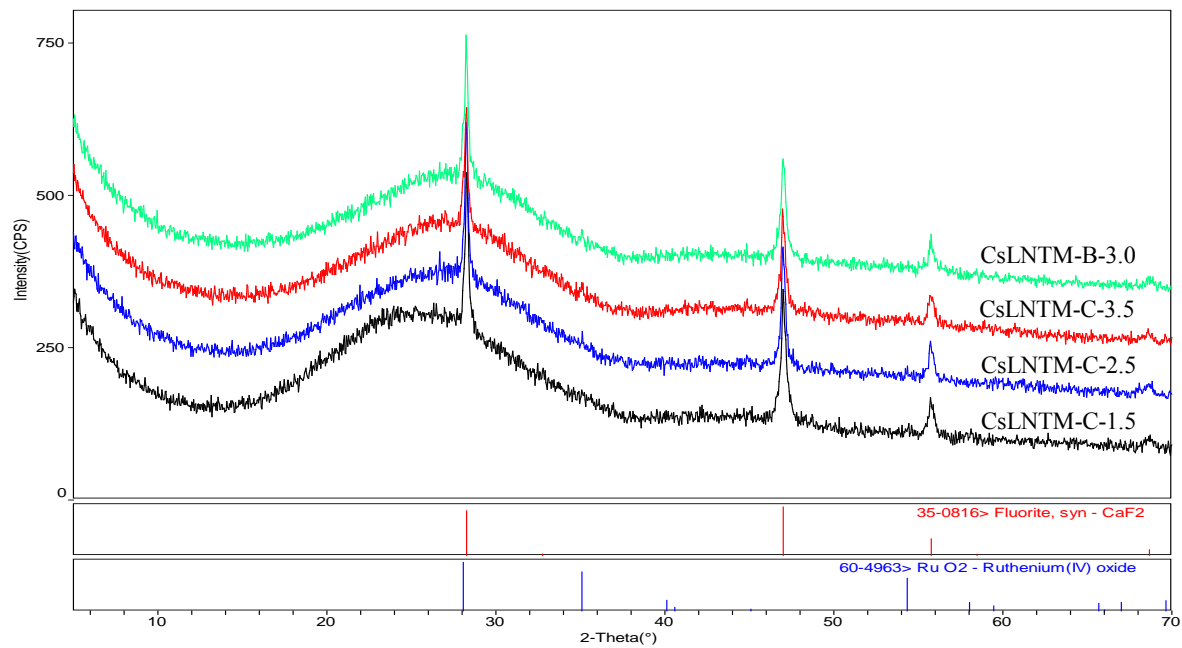


Figure 2 XRD scans of Option 1 glasses with fluorite internal standard.

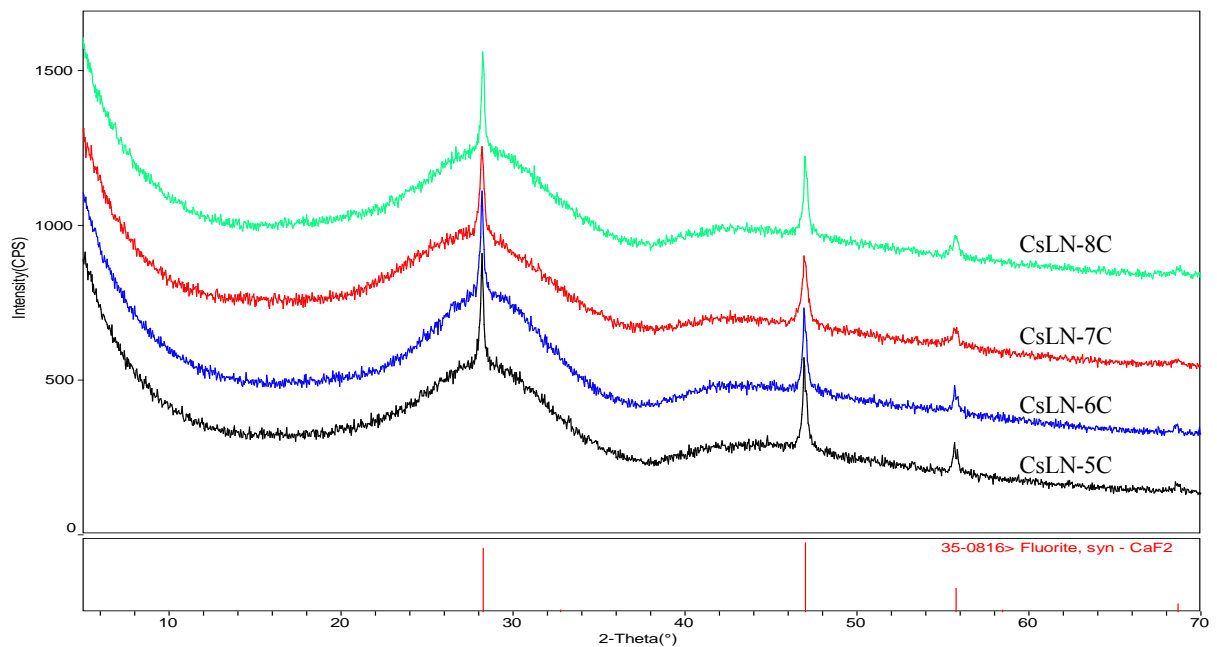


Figure 3 XRD scans of Option 2 glasses with fluorite internal standard.



## 4.2 Slow Cooled Glasses

All of the glasses were slow cooled following the cooling schedule shown in Table 4 to simulate the estimated cooling curve that the glass would experience at the canister centerline. For further information regarding the cooling curve see Appendix A. Figure 4 shows pictures of the top surfaces of each of the Option 1 glasses while still inside the platinum crucibles following the slow cool heat treatment. Visually, all of the Option 1 glasses showed evidence of undissolved noble metals after slow cooling. Glasses CSLNTM-C-1.0 through CSLNTM-C-2.5 are all shiny, transparent and void of other crystalline phases, whereas CSLNTM-C-3.5 and CSLNTM-B-3.0 both have dull, translucent microcrystalline surfaces. All of the Option 2 glasses, except for CSLN-7C were dull, opaque, and microcrystalline at the top surfaces (Figure 5). Glass CSLN-7C was the only Option 2 glass with a shiny or glass-like appearance following the slow cool heat treatment; however like the others it is also opaque.

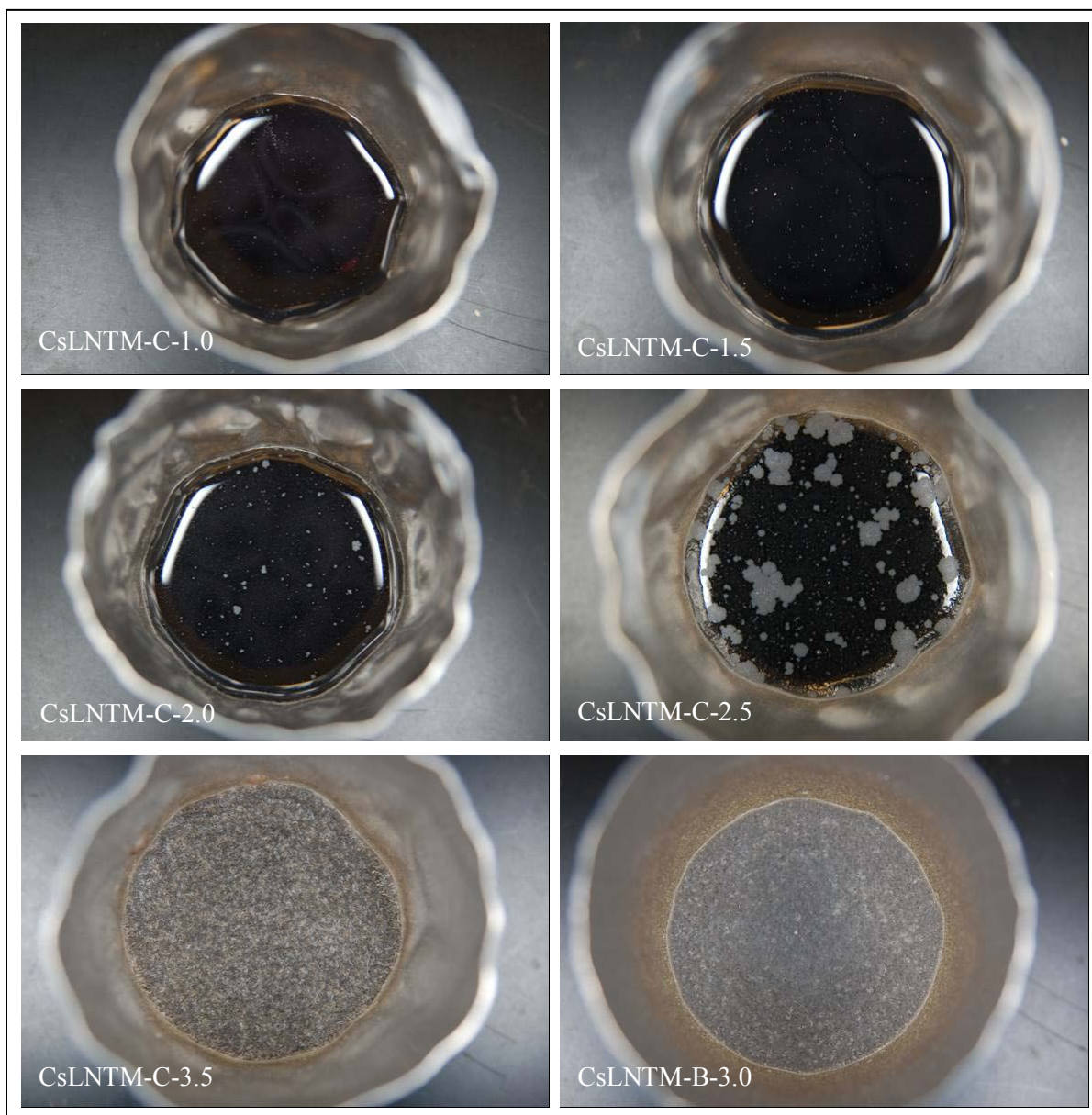


Figure 4 Pictures of Option 1 glasses following slow cooled heat treatment.

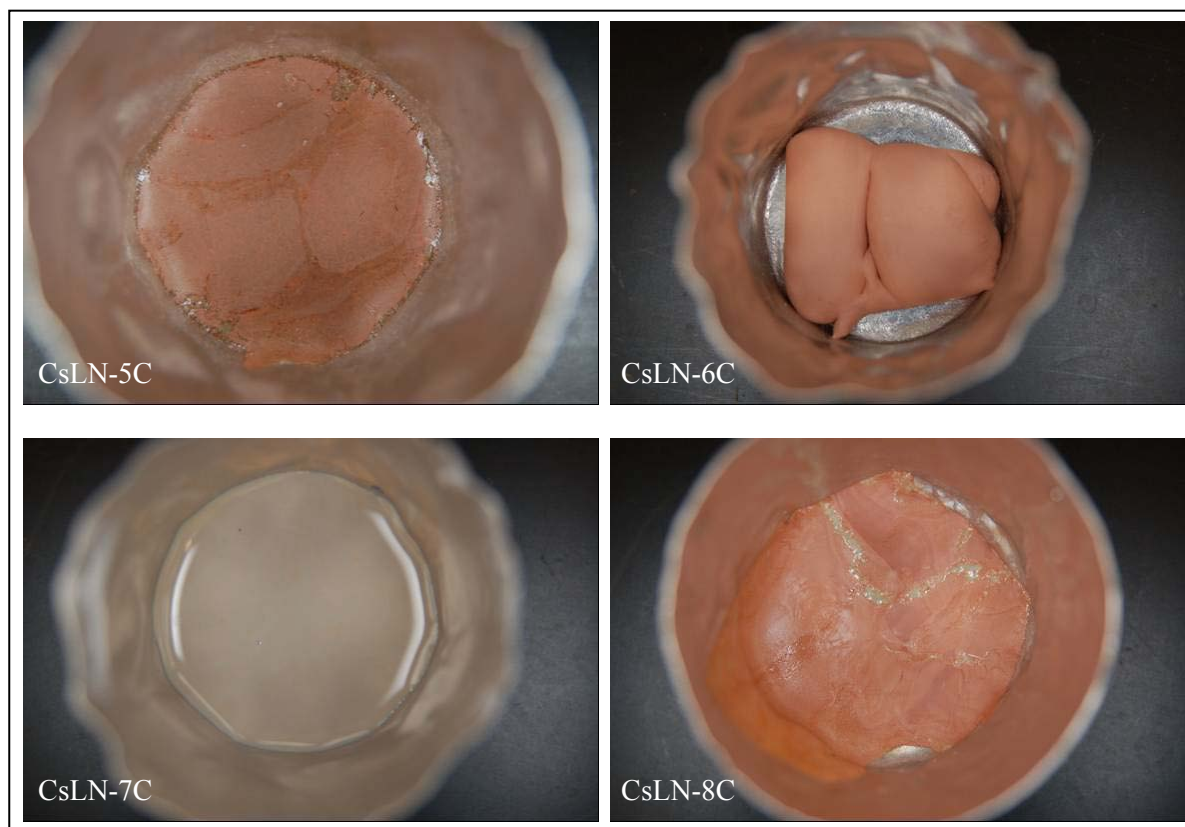


Figure 5 Pictures of Option 2 glasses following slow cooled heat treatment.

An XRD analysis was performed on each of the slow cooled glasses to determine the crystal type and concentration of crystalline phases in the slow cooled glass. The phases identified along with concentrations where quantitative analysis could be done, are given in Table 5.

Table 4 Slow cooling heat treatment schedule

	Start Temperature (°C)	Rate (°C/min)	Step Duration (hours)
1.	1200°C	0	Preheat 0.5 hours
2.	1150°	~ -7	Fast cool
3.	1050°	-0.935	1.8
4.	950°	-0.288	3.7
5.	886°	-0.108	6.3
6.	845°	-0.205	17.8
7.	626°	-0.126	30
8.	400°	0	Dwell 1 hour

Figure 6 shows the XRD patterns of the Option 1 glasses along with identified crystalline phases and corundum internal standard, which was used only when crystallinity was identified. The XRD patterns of the Option 2 glasses and identified crystalline phases are shown in Figure 7. Some of the Option 2

glasses contained phases for which structure files could not be found in the ICSD structure data base or literature. The concentrations of these crystalline phases could not be determined with XRD and were instead qualitatively rated as either a major or minor phase based on height of 100 percent peak for each crystalline phase.

Table 5 Crystalline phases present after slow cooling with quantitative or qualitative concentrations

Glass ID	$\text{Ca}_2\text{Nd}_8\text{Si}_6\text{O}_{26}$	$\text{CsAlSi}_2\text{O}_6$	$\text{BaAl}_2\text{Si}_2\text{O}_8$	$\text{CeO}_2$	$\text{NdBO}_3$	$\text{RuO}_2$	Amorphous
CSLNTM-C-1.0							100
CSLNTM-C-1.5						trace	100
CSLNTM-C-2.0						trace	100
CSLNTM-C-2.5						trace	100
CSLNTM-C-3.5	6.2	0.8				trace	93.0
CSLNTM-B-3.0	7.0					trace	93.0
CSLN-5C		major	major	minor	minor		
CSLN-6C		major	major	minor	minor		
CSLN-7C							
CSLN-8C		major	major	minor	minor		

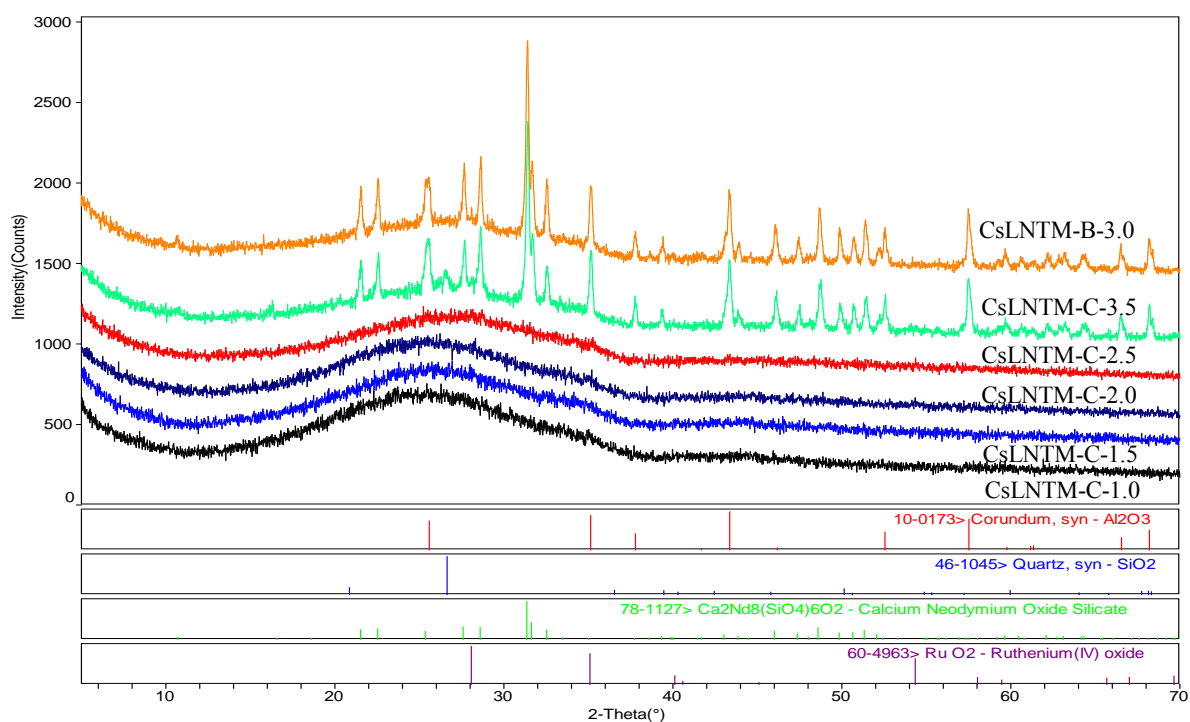


Figure 6 XRD scans of slow cooled Option 1 glasses (corundum,  $\text{Al}_2\text{O}_3$  was used as an internal standard when crystals were present).

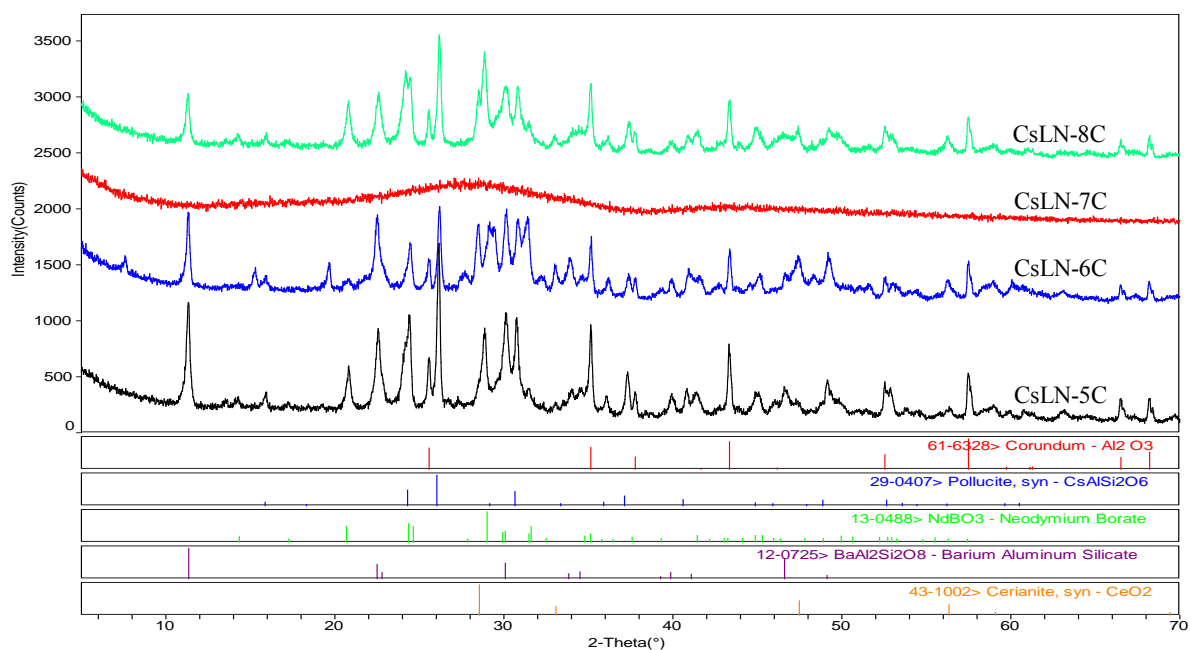


Figure 7 XRD scans of slow cooled Option 1 glasses (corundum, Al<sub>2</sub>O<sub>3</sub> was used as an internal standard when crystals were present).

### 4.3 Chemical Composition Results

The measured and target compositions for the Option 1 and Option 2 glasses are given in Table 6 and Table 7, respectively. The measured compositions of the Option 1 glasses match the target compositions well ( $\pm 1.5$  mass%), with the exception of BaO, and the noble metals which are very low or missing according to the measured compositions. The measurement of the noble metals (PdO, RhO<sub>2</sub>, and RuO<sub>2</sub>) was difficult because these oxides do not dissolve in KOH or Na<sub>2</sub>O<sub>2</sub>. The XRD analysis and OM both show a considerable amount of noble metals were in all of the quenched glasses, in the form of undissolved particles. Barium oxide on the other hand was expected to be measurable by the chemical analysis methods used and was seen in the measurements of the Option 2 glasses. Further compositional analysis will be performed on those glasses that did not contain the targeted BaO concentration and those results will be included in the annual summary report.

The measured compositions of the Option 2 glasses were all near the targeted glass compositions ( $\pm 2.5$  mass%) with the exception of Cs<sub>2</sub>O which measured low in all of the glasses and especially in glasses CSLN-5C, -6C, and -8C. The low concentration of Cs<sub>2</sub>O may indicate volatility of the Cs<sub>2</sub>O during glass melting. The Cs<sub>2</sub>O concentration for CSLN-7C was much closer its targeted composition.

Table 6 Option 1 measured and target glass compositions, mass%

Oxide	CSLNTM-C-1.0		CSLNTM-C-1.5		CSLNTM-C-2.0		CSLNTM-2.5		CSLNTM-C-3.5		CSLNTM-B-3.0	
	Measured	Target	Measured	Target	Measured	Target	Measured	Target	Measured	Target	Measured	Target
Ag <sub>2</sub> O	0.02	0.03	0.05	0.04	0.06	0.06	0.08	0.07	0.10	0.10	0.10	0.11
Al <sub>2</sub> O <sub>3</sub>	10.16	10.00	9.97	9.38	7.02	6.66	6.70	5.95	6.10	5.68	7.20	6.53
B <sub>2</sub> O <sub>3</sub>	10.36	10.00	10.39	9.65	8.89	8.46	5.57	5.00	5.08	5.00	5.59	5.16
BaO	0.48	0.56	0.03	0.85	0.98	1.13	0.06	1.41	0.09	1.98	0.10	2.20
CaO	4.97	5.00	5.32	5.00	4.96	5.00	7.76	7.00	5.38	5.00	5.68	5.16
CdO	0.02	0.03	0.03	0.04	0.05	0.06	0.06	0.07	0.09	0.10	0.10	0.11
CeO <sub>2</sub>	0.78	0.79	1.19	1.19	1.67	1.59	2.01	1.98	2.91	2.78	3.09	3.09
Cs <sub>2</sub> O	0.68	0.74	1.05	1.10	1.41	1.47	1.72	1.84	2.35	2.58	2.58	2.87
Eu <sub>2</sub> O <sub>3</sub>	0.04	0.04	0.06	0.07	0.08	0.09	0.10	0.11	0.14	0.15	0.15	0.17
Gd <sub>2</sub> O <sub>3</sub>	0.04	0.04	0.06	0.06	0.08	0.08	0.11	0.10	0.16	0.15	0.17	0.16
La <sub>2</sub> O <sub>3</sub>	0.33	0.40	0.53	0.61	0.67	0.81	0.89	1.01	1.30	1.42	1.43	1.58
Li <sub>2</sub> O	4.40	4.50	4.40	4.50	4.48	4.50	4.00	4.02	3.22	3.30	3.21	3.21
MoO <sub>3</sub>	0.85	1.00	1.52	1.50	1.69	2.00	2.49	2.50	3.22	3.50	0.72	0.78
Na <sub>2</sub> O	9.26	8.37	8.37	7.00	6.72	6.00	8.36	7.00	8.36	7.00	8.63	7.22
Nd <sub>2</sub> O <sub>3</sub>	1.24	1.34	2.05	2.01	2.50	2.68	3.39	3.36	4.77	4.70	5.26	5.22
PdO	0.00	0.00	0.00	0.01	0.00	0.01	0.00	0.01	0.00	0.02	0.00	0.02
Pr <sub>2</sub> O <sub>3</sub>	0.36	0.37	0.53	0.56	0.72	0.74	0.90	0.93	1.32	1.30	1.47	1.44
Rb <sub>2</sub> O	0.12	0.11	0.16	0.16	0.25	0.22	0.28	0.27	0.40	0.38	0.45	0.42
RhO <sub>2</sub>	0.00	0.02	0.00	0.03	0.00	0.04	0.00	0.05	0.00	0.07	0.00	0.07
RuO <sub>2</sub>	0.00	0.05	0.00	0.08	0.00	0.10	0.00	0.13	0.00	0.18	0.00	0.18
SeO <sub>2</sub>	0.00	0.02	0.00	0.03	0.00	0.04	0.00	0.05	0.00	0.07	0.00	0.08
SiO <sub>2</sub>	55.39	54.93	53.58	53.67	55.71	54.98	54.11	53.03	47.84	48.82	50.71	49.94
Sm <sub>2</sub> O <sub>3</sub>	0.26	0.28	0.38	0.41	0.52	0.55	0.66	0.69	0.93	0.96	1.02	1.07
SnO <sub>2</sub>	0.01	0.02	0.01	0.03	0.03	0.04	0.02	0.04	0.03	0.06	0.03	0.07
SrO	0.27	0.25	0.36	0.38	0.53	0.50	0.63	0.63	0.86	0.88	0.96	0.98
TeO <sub>2</sub>	0.14	0.17	0.22	0.25	0.30	0.34	0.37	0.42	0.51	0.59	0.56	0.65
Y <sub>2</sub> O <sub>3</sub>	0.15	0.16	0.23	0.24	0.31	0.32	0.38	0.40	0.53	0.56	0.59	0.63
ZrO <sub>2</sub>	0.68	0.76	1.04	1.15	1.34	1.53	1.88	1.91	2.70	2.67	0.82	0.87
Total	101.03	100.00	101.54	100.00	100.96	100.00	102.54	100.00	98.41	100.00	100.62	100.00



Table 7 Option 2 measured and target glass compositions, mass%

	CSLN-5C		CSLN-6C		CSLN-7C		CSLN-8C	
Oxide	Measured	Target	Measured	Target	Measured	Target	Measured	Target
Al <sub>2</sub> O <sub>3</sub>	18.58	17.00	19.43	17.00	18.07	17.00	21.57	20.00
B <sub>2</sub> O <sub>3</sub>	10.65	10.00	4.66	5.00	10.50	10.00	10.26	10.00
BaO	7.16	6.98	8.16	7.61	6.02	5.71	7.22	6.98
CeO <sub>2</sub>	8.85	8.61	10.14	9.39	7.77	7.04	9.26	8.61
Cs <sub>2</sub> O	4.90	7.31	3.80	7.97	5.45	5.98	5.10	7.31
Eu <sub>2</sub> O <sub>3</sub>	0.44	0.50	0.52	0.54	0.40	0.41	0.45	0.50
Gd <sub>2</sub> O <sub>3</sub>	0.62	0.57	0.66	0.62	0.48	0.46	0.61	0.57
La <sub>2</sub> O <sub>3</sub>	4.24	4.39	4.76	4.79	3.58	3.59	4.38	4.39
Nd <sub>2</sub> O <sub>3</sub>	14.13	14.50	15.78	15.82	11.34	11.86	13.93	14.50
Pr <sub>2</sub> O <sub>3</sub>	4.18	4.00	4.79	4.37	3.26	3.28	4.18	4.00
Rb <sub>2</sub> O	0.87	0.94	0.82	1.02	0.79	0.77	0.92	0.94
SiO <sub>2</sub>	19.58	18.00	20.19	18.00	29.48	28.00	15.85	15.00
Sm <sub>2</sub> O <sub>3</sub>	3.04	3.04	3.56	3.32	2.59	2.49	3.16	3.04
SrO	2.52	2.41	2.82	2.63	2.09	1.98	2.58	2.41
Y <sub>2</sub> O <sub>3</sub>	1.84	1.75	2.11	1.91	1.44	1.43	1.80	1.75
Total	101.59	100.00	102.20	100.00	103.27	100.00	101.28	100.00

#### 4.4 PCT Results

The PCT results for Option 1 glasses (combined CS/LN/TM waste streams) are shown in Table 8. The elements Li, B, and Na are generally considered good indicators of bulk glass dissolution whereas Si is susceptible to precipitation from the leachate solution. Molybdenum was measured to identify if a water-soluble Mo phase was present. The PCT releases of Li, B, Na, and Si for the quenched and slow cooled glasses were all an order of magnitude below those of the EA reference glass. The normalized elemental releases for Mo tracked very closely with other releases, except for CSLNTM-C-3.5-SC, which had a Mo release that was nearly double that of the next highest, Li release. The slow cooled specimen appears to have formed a Mo-rich phase that was preferentially released from this particular glass with the highest concentration of MoO<sub>3</sub>. However, as discussed in section 4.2, no Mo-rich phases were identified from XRD analysis of the slow cooled glasses. It was hypothesized that a Mo-rich immiscible glass phase formed in this sample. Additional characterization is required to confirm. For all other glasses, the slow cooled heat treatment had no noticeable effect on the normalized releases in the PCT data.

Table 8 Measured PCT response for Option 1 quenched and slow cooled glasses  
(Q = quenched or SC = slow cooled)

Glass ID	Normalized elemental release, g/L				
	Li	B	Na	Si	Mo
ARM	0.58	0.50	0.49	0.29	NA
EA	6.55	10.72	8.56	2.99	NA
CSLNTM-C-1.0-Q	0.38	0.19	0.23	0.13	0.12
CSLNTM-C-1.0-SC	0.34	0.17	0.19	0.13	0.10
CSLNTM-C-1.5-Q	0.38	0.19	0.18	0.12	0.14
CSLNTM-C-1.5-SC	0.35	0.16	0.17	0.12	0.12
CSLNTM-C-2.0-Q	0.43	0.26	0.25	0.14	0.23
CSLNTM-C-2.0-SC	0.39	0.21	0.23	0.14	0.20
CSLNTM-C-2.5-Q	0.51	0.21	0.42	0.16	0.22
CSLNTM-C-2.5-SC	0.47	0.19	0.35	0.15	0.20
CSLNTM-C-3.5-Q	0.61	0.30	0.50	0.18	0.30
CSLNTM-C-3.5-SC	0.58	0.15	0.40	0.11	1.06
CSLNTM-B-3.0-Q	0.49	0.25	0.42	0.15	0.17
CSLNTM-B-3.0-SC	0.52	0.18	0.41	0.15	0.12

The PCT results for the Option 2 glasses (combined CS/LN waste streams) are shown in Table 9. The normalized releases of B, Si, and Al were measured because Li and Na are absent from the Option 2 glasses. The normalized releases of the quenched and slow cooled glasses were two orders of magnitude below the EA glass, with the exception of CSLN-6C-SC, which had an elevated release for B; but even so, that was still approximately an order of magnitude below the EA glass. The slow cooled glasses that crystallized had at least a slightly higher B release than those of the quenched glasses, while Si and Al both are lower for the slow cooled glasses. The higher B release may be attributed to the lanthanide borate ( $\text{NdBO}_3$ ) crystalline phase in the slow cooled glasses identified with XRD. Borates are generally considered less durable than silicates. The increased B release was still well below that of the EA glass and thus not considered to be problematic.

Table 9 Measured PCT response for Option 2 quenched and slow cooled glasses  
(Q = quenched or SC = slow cooled)

Glass ID	Normalized elemental release, g/L		
	B	Si	Al
ARM	0.50	0.29	NA
EA	10.72	2.99	0.09
CSLN-5C-Q	0.03	0.04	0.04
CSLN-5C-SC	0.10	0.02	0.02
CSLN-6C-Q	$\leq 0.01^A$	0.02	0.02
CSLN-6C-SC	1.44	0.02	0.12
CSLN-7C-Q	0.04	0.02	0.01
CSLN-7C-SC	0.02	0.03	0.02
CSLN-8C-Q	0.05	0.02	0.03
CSLN-8C-SC	0.40	0.03	0.04

<sup>A</sup> reported as lower detection limit of ICP-AES analysis.

## 4.5 Liquidus Temperature

Liquidus temperatures of the glasses were measured by a combination of the optical method (optical  $T_L$ ) and crystal fraction methods (XRD  $T_L$ ), and the results are given in Table 10. The optical  $T_L$  is estimated between the lowest temperature at which the material is amorphous ( $T_A$ ) and highest temperature at which the material contains crystals ( $T_C$ ). To determine  $T_L$  by the crystal fraction method, a series of heat treatment samples at temperatures below  $T_L$  were examined with XRD to determine the fraction of each crystalline phase as a function of temperature. These data for each crystalline phase were fit to a straight line and extrapolated to  $T_L = 0$  mass% crystallinity. The slope of the line and the primary phase identified by XRD are given in Table 10.

The  $T_L$  of  $\text{RuO}_2$  was not determined because of its known insolubility in glass. A small fraction of  $\text{RuO}_2$  dissolves into the glass during the melting process (fabrication), which later crystallizes during the heat treatments. However, the vast majority of the  $\text{RuO}_2$  and other noble metals remain undissolved in the glass. The  $\text{RuO}_2$  was observed with OM and XRD in all of the Option 1 glasses at all temperatures. Optically, the presence of undissolved and crystallized  $\text{RuO}_2$  posed difficulties identifying other crystalline phases near  $T_L$ . Figure 8 shows CSLNTM-C-2.5 heat treated at 998°C with  $\text{RuO}_2$ , black irregular shaped particles, and  $\text{Ca}_{2.2}\text{Nd}_{7.8}\text{Si}_6\text{O}_{26}$ , clear needle shaped crystals clustered in the center of the image. Figure 9 shows CSLNTM-C-1.5 heat treated at 850°C, which contained a cluster of clear needles in the center of micrograph. For the Option 2 glasses (CS/LN waste streams) optical  $T_L$  was more straightforward without the presence of undissolved noble metals, as seen in Figure 10.

The crystal fraction method was also used to support the optical  $T_L$  of the Option 1 glasses because the presence of  $\text{RuO}_2$  does not interfere with identification of other crystalline phases. The crystal fraction method was abandoned for CSLNTM-C-1.5 and CSLNTM-C-2.0 glasses because of low crystal fractions at temperatures  $< T_L$ . Glass CSLNTM-C-1.0 was not determined optically or by the crystal fraction methods because no crystals were observed at any of the temperatures  $\geq 800^\circ\text{C}$ , which is well below any foreseeable  $T_L$  constraint that may be implemented. The XRD crystal fraction method was not successful for the Option 2 glasses because several of the crystalline phases observed were not supported by crystal structure data base ICSD or in literature.

Table 10 Optical and XRD measured  $T_L$  of the Option 1 and 2 glasses along with primary crystalline phase<sup>(b)</sup>

Glass ID	$T_A$ , °C	$T_C$ , °C	Optical $T_L$ , °C	XRD $T_L$ , °C	Slope	Primary Phase
CSLNTM-C-1.0	800	NA	$< 800^\circ\text{C}$	NA	NA	NA
CSLNTM-C-1.5	910	899	906	NA	NA	$\text{LnO}_2$
CSLNTM-C-2.0	925	940	932	NA	NA	$\text{LnO}_2$
CSLNTM-C-2.5	1022	1011	1017	1030	-41.51	$\text{Ca}_2\text{Nd}_8\text{Si}_6\text{O}_{26}$
CSLNTM-C-3.5	1100	1088	1094	1122	-27.60	$\text{Ca}_2\text{Nd}_8\text{Si}_6\text{O}_{26}$
CSLNTM-B-3.0	1136	1120	1128	1141	-23.01	$\text{Ca}_2\text{Nd}_8\text{Si}_6\text{O}_{26}$
CSLN-5	1315	1300	1308	NA	NA	$\text{CsAlSi}_2\text{O}_6$
CSLN-6	1400	1392	1396	NA	NA	$\text{CsAlSi}_2\text{O}_6$
CSLN-7	1215	1200	1208	NA	NA	$\text{Nd}_3\text{BSi}_2\text{O}_{10}$
CSLN-8	1315	1300	1308	NA	NA	$\text{CsAlSi}_2\text{O}_6$

(b) NA – not analyzed



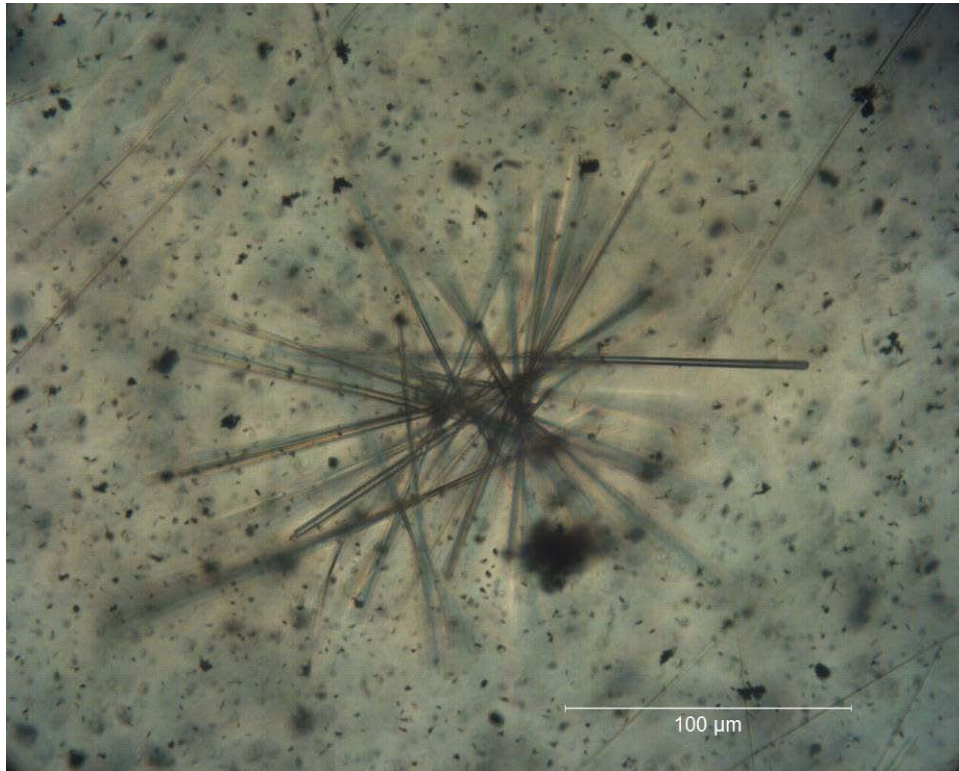


Figure 8 Transmitted light optical micrograph of CSLNTM-C-2.5 at 998°C for 24 hr containing  $\text{Ca}_{2.2}\text{Nd}_{7.8}\text{Si}_6\text{O}_{26}$  (center) and  $\text{RuO}_2$  undissolved particles (throughout).



Figure 9 Transmitted light optical micrograph of CSLNTM-C-1.5 heat-treated at 850°C containing  $\text{Ca}_{2.2}\text{Nd}_{7.8}\text{Si}_6\text{O}_{26}$  (center),  $\text{RuO}_2$  needles and undissolved particles (throughout).

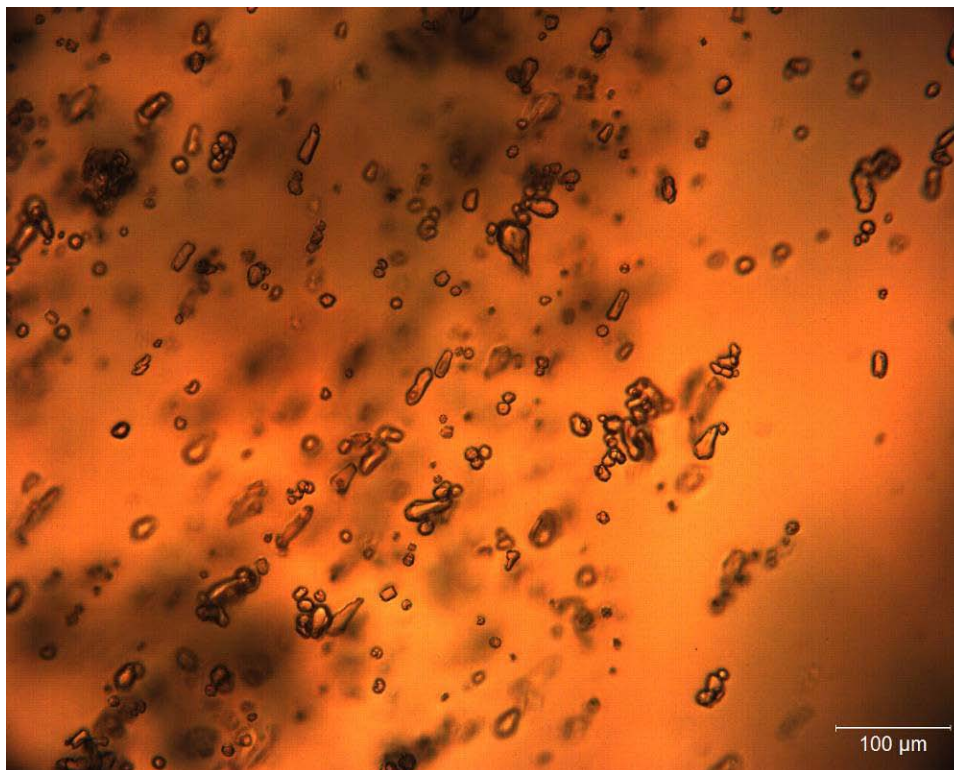


Figure 10 Transmitted light optical micrograph of CSLN-5 heat-treated at 1300°C.

#### 4.6 Measured Glass Density and Glass Transition Temperature

Measured densities and  $T_g$  of the quenched Option 1 and 2 glasses are given in Table 11. Density generally increases with increased waste loading because of the high density of the components in the waste versus the lower density of the glass formers ( $B_2O_3$ ,  $CaO$ ,  $Li_2O$ ,  $Na_2O$ , and  $SiO_2$ ). The  $T_g$  of the Option 1 glasses were all very similar and range from a low of 509°C to a high of 529°C. The  $T_g$  of the Option 2 glasses were considerably higher than the Option 1 glasses because of the large increase in waste loading and low  $SiO_2$  concentrations.

Table 11 Measured densities of Option 1 and 2 glasses

Glass ID	Density, g/cm <sup>3</sup>	$T_g$ , °C
CSLNTM-C-1.0	2.58	515
CSLNTM-C-1.5	2.63	509
CSLNTM-C-2.0	2.68	529
CSLNTM-C-2.5	2.78	515
CSLNTM-C-3.5	2.90	523
CSLNTM-B-3.0	2.89	527
CaLN-5C	3.74	721
CaLN-6C	4.00	776
CaLN-7C	3.36	719
CaLN-8C	3.77	721

## 5. Conclusions

A baseline glass was selected for each of the three limiting conditions:

- 1) High MoO<sub>3</sub> CS + LN + TM waste composition (referred to as Collins-CLT waste composition)
- 2) High noble metals CS + LN + TM waste composition (referred to as Bakel waste composition)
- 3) CS + LN waste composition (referred to as Collins-CL waste composition)

Option 1 glass (CS + LN + TM), CSLNTM-C-2.5, was selected as the baseline glass for the waste limited by high MoO<sub>3</sub>. Measured glass properties are summarized in Table 12. This glass had the highest level of MoO<sub>3</sub> in a glass (2.5 mass%) where phase separation was not observed during glass melting or characterization. Second, though not a requirement but rather preferred, it was also the highest loaded MoO<sub>3</sub> containing glass that did not crystallize upon slow cooling. Lastly, the measured glass properties T<sub>L</sub>, viscosity, electrical conductivity, PCT quenched, and PCT slow cooled were all well within the acceptable range for glass processing and waste form performance.

Option 1 glass, CSLNTM-B-3.0, was selected as the baseline glass for the waste limited by high noble metals. Measured glass properties are summarized in Table 12. This glass was the only high noble metals limited glass fabricated because 3 mass% noble metals was chosen as a preliminary constraint based on melter processing concerns. This was deemed prudent, based on the absence of sufficient data to determine a hard limit. This glass did crystallize 7 mass % of Ca<sub>2</sub>Nd<sub>8</sub>Si<sub>6</sub>O<sub>26</sub> upon slow cooling, but the crystalline phase had no detrimental effect on the waste form performance as tested by the PCT. The measured glass properties T<sub>L</sub>, viscosity, electrical conductivity, PCT quenched, and PCT slow cooled were all well within the acceptable range for glass processing and waste form performance.

Table 12 Summary of measured glass properties

Glass ID	CSLNTM-C-2.5	CSLNTM-B-3.0	CSLN-7C
Quenched crystallinity, mass%	Trace RuO <sub>2</sub>	Trace RuO <sub>2</sub>	0
Slow cooled crystallinity, mass%	Trace RuO <sub>2</sub>	7.0, Ca <sub>2</sub> Nd <sub>8</sub> Si <sub>6</sub> O <sub>26</sub> Trace RuO <sub>2</sub>	0
Optical T <sub>L</sub> , °C	1017	1128	1208
XRD T <sub>L</sub> , °C	1030	1141	NA
Primary crystalline phase	Ca <sub>2</sub> Nd <sub>8</sub> Si <sub>6</sub> O <sub>26</sub>	Ca <sub>2</sub> Nd <sub>8</sub> Si <sub>6</sub> O <sub>26</sub>	NA
Quenched PCT B, g/L	0.21	0.25	0.04
Slow cooled PCT B, g/L	0.19	0.18	0.02
Density, g/cm <sup>3</sup>	2.78	2.89	3.36
T <sub>g</sub> , °C	515	527	719
T <sub>M</sub> , °C	1233	1240	1356
A <sup>(a)</sup>	-8.68	-10.35	-19.00
B <sup>(a)</sup>	15505	18097	33582
ε at T <sub>M</sub> , S/m	20.53	17.21	0.71
C <sup>(b)</sup>	8.42	9.02	17.58
D <sup>(b)</sup>	-8124	-9338	-29201

(a)  $\text{Ln}[\eta, \text{Pa-s}] = A + B/T$

(b)  $\text{Ln}[\epsilon, \text{S/m}] = C + D/T$



Glass, CSLN-7C, was selected as the baseline glass from the Option 2 (CS + LN only) glasses based on its overall properties, which are shown in Table 12. It was the only Option 2 glass tested in this study that did not massively crystallize upon slow cooling. It also had a significantly lower measured  $T_L$  (~1200°C) which was 100-200°C lower than the other three glasses. The low  $T_L$  allows the melter operating temperature to be dropped accordingly, which will generally result in lower  $\text{Cs}_2\text{O}$  volatility and less corrosion of melter refractory, all other things being held constant. The electrical conductivity of this glass was very low in comparison to the Option 1 glasses, because of the low alkali concentration, at 2.66 mole %. All other measured glass properties  $T_L$ , viscosity, PCT quenched and PCT slow cooled are well within the acceptable range for glass processing and waste form performance.

The other three Option 2 glasses tended to massively crystallize upon slow cooling as waste loading was increased. Consequently, the development of a glass-ceramic waste form would be a logical approach to achieve higher waste loading of the combined CS + LN waste streams. If a glass-ceramic was developed that was > 90 mass% crystallized then the heat load would no longer be limited by the  $T_g$  but rather by the much higher melting points of the crystalline phases or the container.

It should be noted that while borosilicate based glass was selected as the baseline glass for this study, that the phosphate glass system is currently being examined by others for the Option 1 high  $\text{MoO}_3$  combined waste stream to determine if it might be a better glass system for high  $\text{MoO}_3$ .

## 6. References

1. Gombert, D., Carter, J., Ebert, W., Piet, S., Trickel, T., and Vienna, J., A Trade Study for Waste Concepts to Minimize HLW Volume, MRS, in press.
2. Bakel, A.J., Bowers, D.L., Quigley, K.J., Regalbuto, M.C., Stillman, J.A., and Vandegrift, G.F. 2006. "Dissolution of Irradiated Nuclear Fuel from the Big Rock Point Reactor." in *Separations for The Nuclear Fuel Cycle in the 21st Century*, ACS Symposium Series **933**, 71-88.
3. Adachi, T., Ohnuki, M., Yoshida, N., Sonobe, T., Kawamura, W., Takeishi, H., Gunji, K., Kimura, T., Suzuki, T., Nakahara, Y., Muromura, T., Kobayashi, Y., Okashita, H., and Yamamoto, T. 1990. "Dissolution Study of Spent PWR Fuel: Dissolution Behavior and Chemical Properties of Insoluble Residues." *Journal of Nuclear Materials*, **174**, 60-71.
4. Pereira, C., Regalbuto, M.C., Vandegrift, G.F., Bakel, A., Basco, J., Bowers, D., Byrnes, J.P., Clark, M.A., Cramer, C., Falkenberg, J.R., Guelis, A.V., Hafenrichter, L., Kalensky, M., Krebs, J.F., Leyva, A., Miller, L., Shroy, B., Sullivan, V., Tsai, Y., Quigley, K.J., and Wright, A. 2006. Preliminary Results of the UREX+1a Spent Fuel Process Demonstration. Argonne National Laboratory Letter Report, September 30, 2006. (Official Use Only)
5. Collins, E., Testing Results CETE, Waste Forms – TMFP Composition Video Conference, November 19, 2008
6. UREX+ Waste Composition Variability Analysis, J. V. Crum, J. V. Ryan, J. D. Vienna, AFCI-WAST-WAST-MI-DV-2009-000076, 2009
7. Olson, K. M. *Fabrication and Leaching of West Valley Demonstration Project Glasses: Ten Quarter 2 and Ten Quarter 3 Glasses*; Pacific Northwest National Laboratory: Richland, WA, 1993.
8. Jantzen, C. M.; Pickett, J. B.; Brown, K. G.; Edwards, T. B.; Beam, D. C. *Process/Product Models for the Defense Waste Processing Facility (DWPF): Part I. Predicting Glass Durability from Composition Using a Thermodynamic Hydration Energy Reaction Model (THERMO)*; WSRC-TR-93-0672; Savannah River Technology Center: Aiken, SC, 1993.
9. Fu, S. S.; Pegg, I. L. *Glass Formulation and Testing with TWRS HLW Simulants, VSL Final Report*. The Catholic University of America: Washington, D.C., 1998.

10. Day, D. E., Ray, C. S., Kim, C. W., Iron Phosphate Glasses: An Alternative For Vitrifying Certain Nuclear Wastes, Final Report for DE-FG01-96ER45618, University of Missouri-Rolla, Rolla, MO, 2004
11. Vienna, J. D., Schweiger, M. J., Riley, R. J., Smith, D. E., Peeler, D. K., Reamer, I. A., *Property Data for Simulated Americium/Curium Glasses*, PNNL-13009, October 1999.
12. Peeler, D. K., Edwards, T. B., Reamer, I. A., Vienna, J. D., Smith, D. E., Schweiger, M. J., Riley, B. J., Crum, J. V., *Composition/Property Relationships for the Phase 1 Am/Cm Glass Variability Study (U)*, WSRC-TR-99-00055 Rev.0, 1999.
13. Peeler, D. K., Edwards, T. B., Rudisill, T. S., Reamer, I. A., Vienna, J. D., Smith, D. E., Schweiger, M. J., Riley, B. J., *Composition/Property Relationships for the Phase 2 Am/Cm Glass Variability Study (U)*, WSRC-TR-99-00393 Rev.0, October 1999.
14. Riley, B. J., Vienna, J. D., Schweiger, M. J., Peeler, D. K., and Reamer, I. A., Liquidus Temperature of Rare-Earth-Alumino-Borosilicate Glasses for Treatment of Americium and Curium, *Mat. Res. Soc. Symp. Proc.*, **608**, pp. 677-682, January 2000.
15. Crum, J. V. and Vienna, J. D., Glasses for Immobilizing Lanthanide, Alkali, Alkali-Earth Fission Products, MS&T2008, David Lawrence Convention Center, Pittsburgh, PA, in press.
16. "Glass Batching and Melting," Pacific Northwest National Laboratory (PNNL), Richland, WA, Report No. Technical Procedure GDL-GBM, Rev. 3.
17. A – SRNL, "Sample Dissolution Using Potassium Hydroxide Fusion" Savannah River National Laboratory, Aiken, SC, Report No. SRTC Procedure Manual, L29, ITS-00035.
18. B – SRNL, "Lithium Metaborate Fusion Preparation" Savannah River National Laboratory, Aiken, SC, Report No. SRTC Procedure Manual, L29, ITS-00071."
19. C – SRNL, "Inductively Coupled Plasma-Atomic Emission Spectrometer Varian Vista AX" Savannah River National Laboratory, Aiken, SC, Report No. SRTC Procedure Manual, L29, ITS-00079.
20. "Standard Test Methods for Determining Chemical Durability of Nuclear, Hazardous, and Mixed Waste Glasses and Multiphase Glass Ceramics: The Product Consistency Test (PCT)," West Conshohocken, PA, Report No. ASTM C-1285-2002.
21. "Operation of Scintag Pad-V X-Ray Diffractometer," Pacific Northwest National Laboratory (PNNL), Richland, WA, Report No. Technical Procedure APEL-XRD-1, Rev. 0.
22. "Standard Test Methods for Determining the Liquidus Temperature ( $T_l$ ) of Waste Glasses and Simulated Waste Glasses," Pacific Northwest National Laboratory (PNNL), Richland, WA, Report No. Technical Procedure GDL-LQT, Rev. 4.
23. "Density Measurements of Solids Using the Accupyc® Gas Pycnometer," Pacific Northwest National Laboratory (PNNL), Richland, WA, Report No. Technical Procedure GDL-PYC, Rev. 2.
24. "Standard Test Method for Assignment of the Glass Transition Temperatures by Differential Scanning Calorimetry," West Conshohocken, PA, Report No. ASTM E-1356-08.
25. "Standard Test Method for Assignment of the Glass Transition Temperature by Thermomechanical Analysis," West Conshohocken, PA, Report No. ASTM E-1545-05
26. "Standard Viscosity Measurement Procedure for Vitrified Nuclear Waste," Pacific Northwest National Laboratory (PNNL), Richland, WA, Report No. Technical Procedure GDL-VIS, Rev. 1.
27. Waste/Storage Form Baseline-Fission Products & Lanthanides, A. L. Youchak-Billings, J. V. Crum, J. C. Marra, B. J. Riley, J. D. Vienna, and A. Edmondson, GNEP-WAST-PMO-MI-DV-2008-000151, 2008

## **Appendix A**

### **Slow Cooling Heat Treatment Curve**

The following work was done to establish a canister centerline cooling curve for testing of AFCI glass waste forms. An established slow cooling curve is available to simulate the centerline cooling curve of a Waste Treatment Plant (WTP) high level waste (HLW) glass canister.<sup>[1,2]</sup> However the heat will be significantly higher in an AFCI glass waste form than a HLW glass waste form because of the increased concentrations of Cs and Sr isotopes. A heat value of 14,000 watts/canister was chosen to develop a centerline cooling curve for AFCI combined fission products glass. Modeling of the cooling curve was done with and without heat to determine the effect on centerline cooling rate. Modeling of the cooling curve with heat was deemed to be overly conservative. Instead the difference between the two modeled cooling curves, with and without heat, were tabulated (Table A1) and added to the documented centerline cooling curve previously established for WTP HLW canisters. Table A2 shows the WTP established cooling curve and the curve adjusted for added heat.

Table A1. Model generated centerline temperatures of canister assuming no heat, heat and the tabulated difference.

No Heat		With Heat		Difference	
Hours	h = 96"	Hours	h = 96"	Hours	h = 96"
0	872.23	0	872.23	0	0.00
1	870.46	1	881.63	1	11.17
2	865.43	2	887.77	2	22.34
3	857.47	3	890.95	3	33.49
4	843.91	4	888.46	4	44.55
5	823.66	5	879.08	5	55.42
6	797.66	6	863.68	6	66.02
7	767.59	7	843.92	7	76.33
8	735.09	8	821.39	8	86.30
9	701.48	9	797.37	9	95.89
10	667.68	10	772.77	10	105.09
12	601.93	12	724.25	12	122.32
14	540.58	14	678.75	14	138.17
16	484.67	16	637.34	16	152.67
18	434.24	18	600.23	18	165.98
20	388.97	20	567.19	20	178.23
22	348.17	22	537.94	22	189.76
24	311.67	24	512.09	24	200.42
26	279.04	26	489.28	26	210.24
28	249.90	28	469.16	28	219.26
30	223.98	30	451.42	30	227.44
35	171.01	35	415.73	35	244.72
40	131.63	40	389.67	40	258.04
45	102.65	45	370.68	45	268.03
50	81.25	50	356.88	50	275.63
55	65.50	55	346.87	55	281.37
60	53.95	60	339.61	60	285.66

Table A2. Raw WTP HLW cooling curve and heat adjusted centerline cooling curve.

Time (hr)	Raw Curve	Adjusted Curve
0.00	1005	1003
0.75	982	990
1.00	974	985
1.78	951	971
2.00	944	967
3.00	916	950
3.33	906	944
4.00	888	933
5.00	861	917
5.48	848	909
6.00	835	901
7.00	810	886
8.00	785	871
8.78	766	860
9.00	761	857
10.00	738	843
11.00	716	829
11.78	698	818
12.00	694	816
13.00	673	803
14.00	652	790
15.00	633	778
16.00	613	766
17.00	595	754
18.00	577	743
19.00	559	731
20.00	542	721
21.00	526	710
22.00	510	700
23.00	494	690
24.00	479	680
25.00	465	670
26.00	451	661
27.00	437	652
28.00	424	643
29.00	411	634
29.60	403	629
30.00	398	626
31.00	386	617
32.00	374	609
33.00	363	601
34.00	352	593
35.00	341	586
36.00	331	579
37.00	321	571
38.00	311	564



Time (hr)	Raw Curve	Adjusted Curve
39.00	302	557
40.00	293	551
41.00	284	544
42.00	275	538
43.00	267	531
44.00	259	525
45.00	251	519
46.00	243	513
47.00	236	507
48.00	229	502
49.00	222	496
50.00	215	491
51.00	208	486
52.00	202	480
53.00	196	475
54.00	190	470
55.00	184	466
56.00	179	461
57.00	173	456
58.00	168	452
59.00	163	447
60.00	158	443

## References

1. RPP Pilot Melter Prototypic LAW and HLW Canister Glass Fill Test Results Report", TRR-PLT-080, Duratek Inc., April 27, 2004
2. "Canister Centerline Cooling Data, Rev. 1", RPP-WTP Memorandum, R10152486, October 29, 2003